

# Wood stabilisation Using Methyl Methacrylate Polymerisation in the Context of Musical Instrument Making

Romain VIALA<sup>1\*</sup>, Jérémy CABARET<sup>2</sup> and Nicolas MICHAUD<sup>2</sup>

<sup>1\*</sup>Université Marie et Louis Pasteur, CNRS, institut FEMTO-ST (UMR 6174), F-25000, Besançon, France.

<sup>2</sup>Institut Technologique Européen des Métiers de la Musique, ITEM, F-72000, Le Mans, France.

\*Corresponding author(s). E-mail(s): [romain.viala@femto-st.fr](mailto:romain.viala@femto-st.fr);  
Contributing authors: [jeremy.cabaret@itemm.fr](mailto:jeremy.cabaret@itemm.fr);  
[nicolas.michaud@itemm.fr](mailto:nicolas.michaud@itemm.fr);

## Abstract

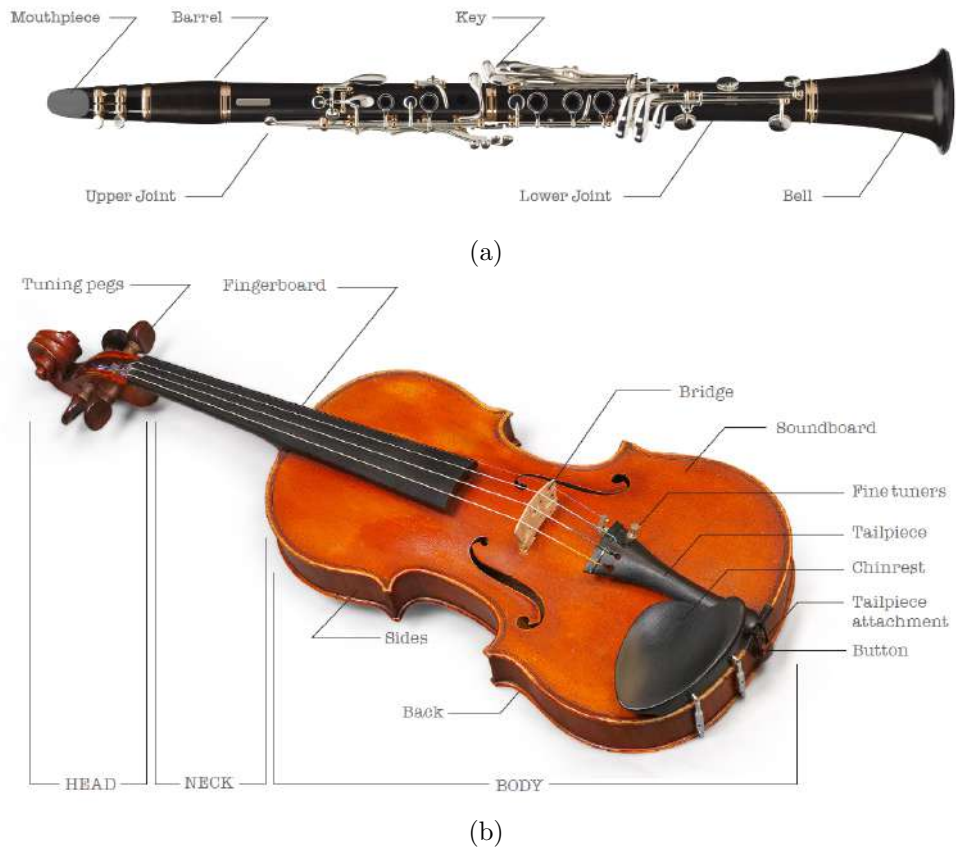
This paper investigates the potential of wood stabilisation techniques in improving the mechanical and acoustical properties of temperate wood species to make them suitable for musical instrument making. Many instruments or parts are usually made with tropical woods, specifically woodwind instruments and fingerboards. For these applications, the wood must be stable, with low porosity and good machinability. The increasingly strict regulations on international trade of vulnerable species reduce the availability of such species. Therefore, a wood stabilisation process using methyl methacrylate impregnation is proposed, focusing on these specific domain criteria. This aims to achieve properties approaching those of African blackwood (*Dalbergia melanoxylon*) used for clarinet and oboes, and African ebony (*Diospyros crassiflora*) used for chordophones fingerboards. Ten different temperate wood species and six specimens (tubes) per species were tested with this process. The Shore-D hardness, hygroscopic behaviour of wood through roundness, moisture exclusion efficiency and anti-swelling efficiency, the acoustic loss factor of the cavity and the density of samples were compared before and after stabilisation. The results suggest that hornbeam (*Carpinus betulus*), maple (*Acer spp.*) and beech (*Fagus sylvatica*) can be used as stabilised materials, for several applications, with improved properties. Generally, the density and hardness are significantly improved and acoustic loss factors and swelling are reduced, to reach values suitable for instrument making, whilst not reaching absolute values of tropical reference woods.

**Keywords:** Wood stabilisation, Woodwind instruments, Wood mechanics, Instrument making, Input impedance

## 1 Introduction

Wood remains one of the dominant materials for the construction of musical instruments, where making, stability, and playability depend strongly on its mechanical and hygroscopic behaviour. For applications such as chordophones fingerboards and woodwind instruments, makers traditionally select woods that combine high hardness, low porosity, dimensional stability, and good machinability. For wind instruments, a smooth and airtight bore (internal dimensions of the instrument) is essential to avoid energy losses and frequency drift (Chaigne and Kergomard 2016; Boutin et al. 2017; Wolfe et al. 2001). For fingerboards, a smooth and stiff material is required, especially when frets are press-fitted into the wood, and modern instruments using metallic strings require woods with high resistance to wear in the fingerboards. Among species, African blackwood (*Dalbergia melanoxylon*) is the wood used for barrel, upper and lower joint and bell of the clarinet for example, as shown in Figure 1 (a). African ebony (*Diospyros crassiflora*) is the most used for quartet instruments fingerboards as shown in Figure 1 (b), but also for guitars. Both woods fulfil these requirements through their high density, low permeability, and low hygroscopicity (Alkadri et al. 2020; Bucur 2006).

**Figure 1:** Nomenclature of the clarinet (ITEMM and CSFI 2020) and the violin (ITEMM and CSFI 2021). Dark parts are generally made with *Dalbergia melanoxylon* for the clarinet and *Diospyros crassiflora* for the violin.



Since 2017, all *Dalbergia* species have been listed in Appendix II of the CITES convention, restricting international trade and encouraging the search for sustainable alternatives (Convention On International Trade In Endangered Species Of Wild Fauna And Flora (CITES) 2016; Calvano et al. 2023). Moreover, since 2019, *Diospyros crassiflora* is in the red list of IUCN in the vulnerable category (Schatz et al. 2019). This regulatory pressure, combined with the rising cost and ecological impact of tropical timbers, has stimulated research on temperate alternatives and on modification methods that can reproduce the functional properties of tropical woods (Sandberg et al. 2017; Jones and Sandberg 2020; Zelinka et al. 2022).

Wood modification strategies aim to improve dimensional stability, hardness, or durability while preserving machinability and structural integrity. They include thermal, chemical, and polymer-impregnation treatments (Hill 2006; Sandberg et al. 2017). For musical applications, such processes must remain compatible with workshop practice, maintain dimensional tolerances, and avoid degrading features of interest in this

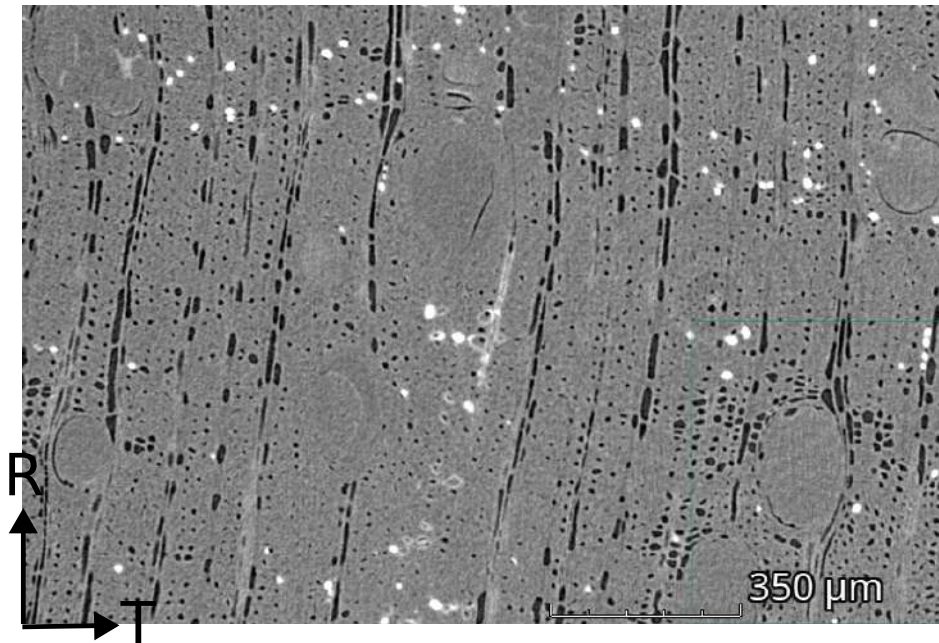
context. Among these methods, impregnation and *in-situ* polymerisation of methyl methacrylate (MMA) have attracted particular attention. MMA-based products have a low-viscosity (typical viscosity for CACTUS JUICE® is 4-6 cP (TurnTex, LLC 2024)) that can penetrate cell lumen and polymerise into poly(methyl methacrylate) (PMMA), yielding a transparent, hard, and dimensionally stable polymer associated with wood by filling porosities (Hu et al. 2013; Stolf et al. 2017; Acosta et al. 2020; Yang et al. 2022; Ding et al. 2008; Gibiat et al. 2007).

Several studies report that MMA impregnation increases density, reduces swelling, and decreases equilibrium moisture content in various hardwoods and softwoods (Ding et al. 2012; Hadi et al. 2019; Priadi et al. 2020; Kim et al. 2020). These effects are generally linked to lumen filling and polymer anchorage in the cell wall, which shorten moisture diffusion paths and improve dimensional stability. Nevertheless, the consequences of such treatments for acoustic features of bores, their airtightness and hardness remain under explored, especially in the context of musical instrument making where multiple criteria coexist.

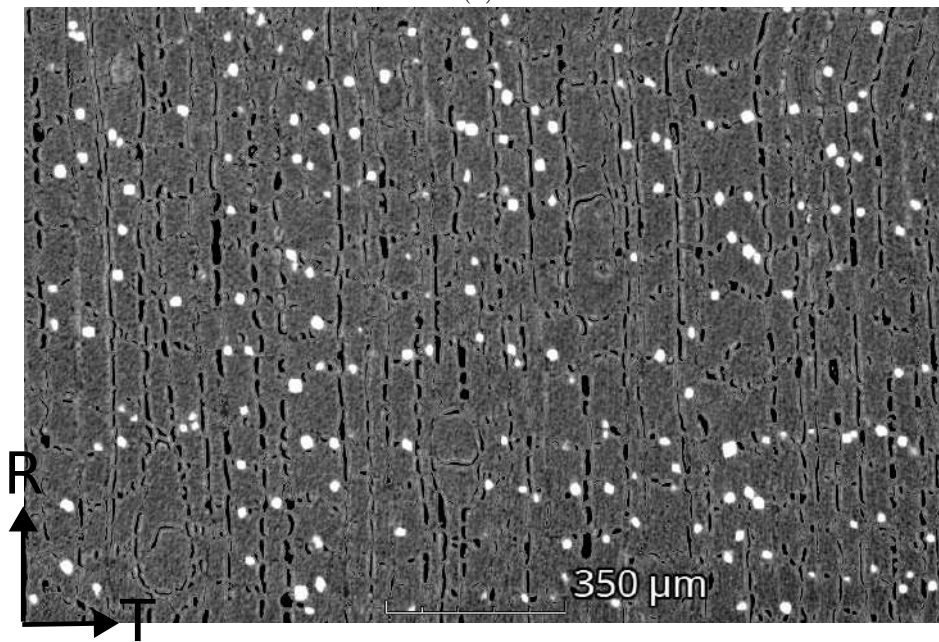
In particular, the relationships between pore filling, dimensional stability, hardness, and air-column acoustic losses have rarely been quantified. Prior work mainly focuses on weight percent gain (WPG) or mechanical moduli, but seldom correlates these with parameters directly affecting playability such as impedance-derived loss factors (Boutin et al. 2017; Wolfe et al. 2001; Dalmont and Le Roux 2008; Ablitzer 2021).

The objective of this work is to evaluate the potential of MMA-based stabilisation as a feasible process for enhancing the physical and acoustic properties of temperate woods for instrument making, and investigate the structure–property relationships underlying these modifications. The MMA under vacuum impregnation and polymerisation is applied to ten temperate wood species common in mainland Europe: *Acer* spp., *Carpinus betulus*, spalted *Fagus sylvatica*, *Fraxinus excelsior* (tested with three commercial resins), *Platanus hispanica*, *Prunus avium*, *Robinia pseudoacacia*, *Olea europaea*, *Cedrus atlantica*, and *Sequoia sempervirens*. Two tropical references widely used by makers, *Dalbergia melanoxylon* and *Diospyros crassiflora*, are included for benchmarking and their microstructure is represented in the Figure 2 (a) and (b), respectively.

**Figure 2:** Tomographic imaging of top: *Dalbergia Melanoxyton*, bottom: *Diospyros crassiflora* in transverse plane (RT).



(a)



(b)

Before and after stabilisation, samples will be characterised under controlled relative humidities (30,50, and 80%), measuring density, Shore-D hardness, equilibrium moisture content, anti-swelling and moisture exclusion efficiency and acoustic loss factors derived from impedance tests. For the most promising temperate woods, X-ray microtomography is used to quantify the reduction of open porosity and the degree of polymer filling. These descriptors directly reflect maker-relevant criteria such as dimensional stability, wear resistance, bore smoothness, and mass.

The remainder of this paper is organised as follows. Section 2 details the wood species, stabilisation protocol and experimental methods used to quantify density, hygroscopic response, dimensional stability, hardness, acoustic loss factors and microstructural changes. Section 3 presents the main results for all temperate and reference species. Section 4 discusses the underlying structure–property relationships, limitations of the current state of knowledge and implications for sustainable instrument manufacture. Finally, Section 5 concludes this work and outlines perspectives for future developments and applications in musical instrument making.

## 2 Materials and Methods

### 2.1 Wood species and sample preparation

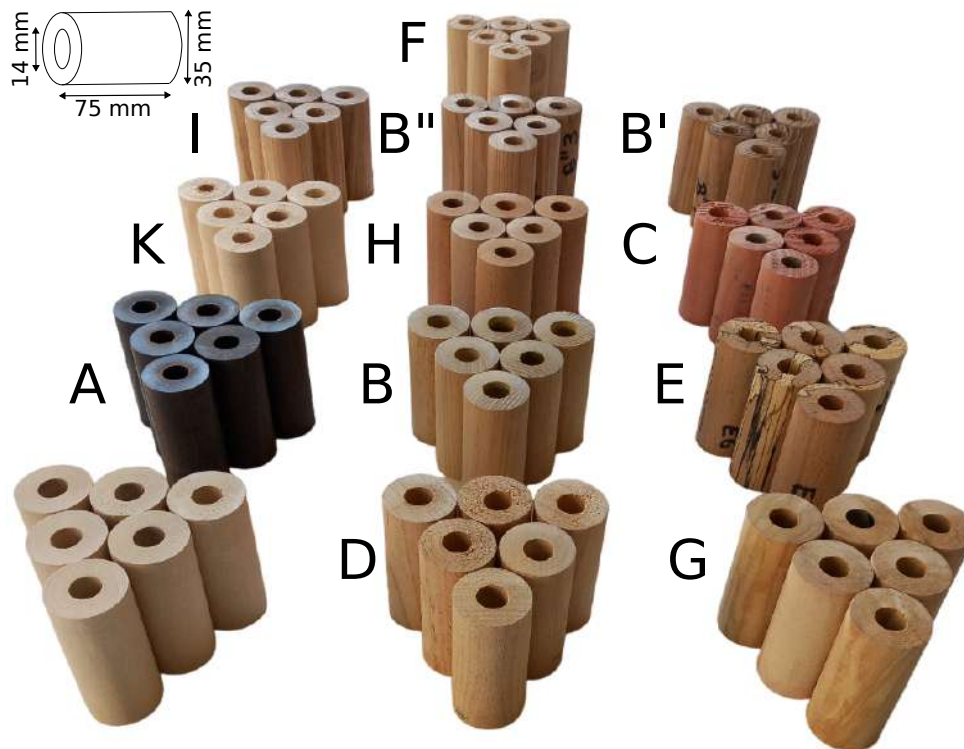
The wood species selected for the experimental campaign grow in mainland France. In total, ten wood species were chosen to highlight inter-specific diversity. Both softwood and hardwood species were selected, including species with varying density. In addition to these species, *Dalbergia melanoxylon* was tested as a reference for woodwinds for comparison with the selected wood species. For fingerboards applications, *Diospyros crassiflora* was tested. Three wood blocks per species (50 × 50 × 200 mm) were ordered from the online retailer *FTFI*, a specialised supplier for woodworking. The selected wood species are described in Table 1.

**Table 1:** Tested wood species and experimental conditions, six samples were prepared for each species, whose identifier is given by  $i$  subscript.

Species and label	Vernacular name	Stabilising product
<i>Dalbergia melanoxylon</i> $A_i$	African blackwood	Not stabilised
<i>Fraxinus excelsior</i> L. $B_i$	European ash	Cactus Juice®
<i>Fraxinus excelsior</i> L. $B'_i$	European ash	NovaCure®
<i>Fraxinus excelsior</i> L. $B''_i$	European ash	StabiCure®
<i>Sequoia sempervirens</i> D.Don $C_i$	Coast redwood	Cactus Juice®
<i>Prunus avium</i> L. $D_i$	Wild cherry	Cactus Juice®
<i>Fagus sylvatica</i> L. spalted $E_i$	Beech	Cactus Juice®
<i>Cedrus atlantica</i> Endl. $F_i$	Atlas cedar	Cactus Juice®
<i>Olea europaea</i> L. $G_i$	Olive tree	Cactus Juice®
<i>Platanus x hispanica</i> Mill. ex Münchh $H_i$	Hybrid plane	Cactus Juice®
<i>Robinia pseudoacacia</i> L. $I_i$	Black locust	Cactus Juice®
<i>Carpinus betulus</i> L. $J_i$	European hornbeam	Cactus Juice®
<i>Acer spp.</i> $K_i$	Maple	Cactus Juice®
<i>Diospyros crassiflora</i> L. $L_i$	African ebony	Not stabilised

The subscript  $i$  indicates the sample number and takes values from 1 to 6. The set of samples obtained is shown in Figure 3. The samples dimensions were chosen to closely resemble a clarinet part called the barrel, with the ultimate goal of transforming the samples into barrels, cut into 90 mm pieces and then turned using a metal lathe to an external diameter of 35 mm. This transformation involves several steps: centring the samples using a drill press, facing, cutting, facing the sides, and drilling the bore along the longitudinal direction. The bore was created using a 14 mm diameter drill bit. The tangential and radial directions were evaluated using circumferential rings. 90 95

**Figure 3:** Experimental samples by wood species, detailed in Table 1, machined as cylindrical tubes.



The samples were stabilised with three types of methyl methacrylate based stabilisation resins, *CACTUS JUICE*® provided by *TURNTTEX*<sup>1</sup>, *NOVACURE*® provided by *DICTUM GmbH*<sup>2</sup> and *STABICURE*® provided by *RESION*<sup>3</sup>. These different references are commonly used for stabilisation and are composed of hydroxyalkyl methacrylate, triethylene glycol dimethacrylate and polyethyleneglyceryl 100

<sup>1</sup><https://turnttx.com>

<sup>2</sup><https://www.dictum.com>

<sup>3</sup><https://polyestershoppen.fr>

oleates in various proportions, not specified by the providers. They can be safely handled using normally accepted practices for handling non-toxic industrial chemicals, such as wearing gloves to avoid skin irritation and protect eyes. Such treatment is employed in contexts where high dimensional stability and long-term durability are required, including decorative and luxury items, knife handles, and various technical components exposed to fluctuating environmental conditions. This product is therefore representative of the stabilisation techniques already adopted in craftsmanship field.

## 2.2 Methods

The samples were then prepared following stabilisation process described below and different physical parameters were defined, also described after. The parameters and associated acronyms are given in the table 2 and measured at 0, 30, 50 and 80% relative humidity.

**Table 2:** Measured and estimated parameters, corresponding acronyms

Measured Variable	Acronym
Equilibrium density at a given relative humidity $RH$ [ $\frac{kg}{m^3}$ ]	$\rho_{RH}$
Tangential shrinkage [ $mm$ ]	$\Delta_T$
Radial shrinkage [ $mm$ ]	$\Delta_R$
$\frac{T}{R}$ ratio [-] ( $\frac{\Delta_{Trel}}{\Delta_{Rel}}$ )	$\frac{T}{R}$
Shore-D hardness [-]	Shore-D
Wood equilibrium moisture content at given $RH$ [-] (%)	$EMC_{RH}$
Acoustic loss factor [-]	$\eta$
Longitudinal elastic modulus [GPa]	$E_L$
Weight percent gain [-] (%)	WPG
Moisture exclusion efficiency [-] (%)	MEE
Anti-swelling efficiency [-] (%)	ASE

### 2.2.1 Stabilisation Using Methyl Methacrylate Impregnation

Following the suppliers' guidelines, the samples are dehydrated in a *Memmert UF-260* oven at 103°C until the mass variation is negligible ( $< 0.05\%$ ). The obtained mass is taken as the oven-dry mass for subsequent calculations. Then, stabilisation is carried out using a chamber connected to a vacuum pump (approximately -95 kPa gauge). The vacuum is applied until complete degassing of the air contained in the dry samples, which lasts 30 minutes for the size of the samples. After the vacuum phase, there is a resting phase within the liquid resin, for 7 hours, to ensure sufficient absorption. The samples are then drained, wrapped in aluminium foil, and heated in an oven at 93°C for 3 hours, as proposed by the supplier, to polymerise the monomers. The aluminium foil is used to avoid leakages of unpolymerised resin and to superimpose specimens. Following stabilisation, the samples were maintained at a constant temperature of

25°C prior to analysis. The advantage of this setup is its easy reproducibility in a workshop for an craftsman.

### 2.2.2 Air column loss factor

In wind instruments, the sound production is predominantly determined by the vibration of the air column inside the instrument, much more than by the material properties of the tube. The acoustic properties such as pitch and timbre depend on the shape, dimensions, and length of the air column rather than the characteristics of the wood. Nevertheless, the smoothness of the interior surface of the instrument plays a role in the damping of the acoustic cavity resonance (Boutin et al. 2017), and can be evaluated using input impedance (Wolfe et al. 2001). A woodwind instrument can be modelled as an ideal cylindrical or conical resonator. The analogy to such a closed-open tube allows to deduce the theoretical resonance frequencies of the tube, which depend on its length, internal diameter, and mode of vibration, as given in equation 1.

$$f_n = \frac{(2n - 1) \cdot c}{4(L + 0.4 \cdot d)} \quad (1)$$

The frequency  $f_n$  is associated with the mode  $n$ , where  $c$  is the speed of sound in air at 20°C,  $L$  the length of the cylinder and  $d$  the internal diameter of the cylinder. The samples have been measured using an impedance bridge (Dalmont and Le Roux 2008). A swept sine wave is sent in the tube with a piezoelectric patch and two pickups measure pressure differential. The impedance curve displays the ratio between acoustic pressure and acoustic velocity as a function of the frequency. Impedance displays peaks corresponding to the resonance of the tube in closed-open conditions. The acoustic loss factor, expressed as twice the modal damping ratio of the resonance peaks (in %), is determined from input impedance measurements using the *PickPeakingTools* software (Ablitzer 2021). This value is an indicator of the acoustic losses inside the bore, associated with visco-thermal losses due to roughness and porosity. Low acoustic loss factor values are associated with smooth surface state, which is wanted during the making of a woodwind instrument, by polishing the inside with fine grain and linseed oil. The acoustic loss factor of the system, which controls the narrowing or broadening of the resonance peaks, is considered to influence the ease of the sound emission and possibility to make pitch shifts.

### 2.2.3 Hardness

The Shore-D hardness scale is one of the most affordable and reliable methods (Esteves 2021). It provides information about the wood resistance to local indentation. In the context of instrument making this property is crucial. For example, when in contact with metals like frets on a guitar fingerboard, the wood needs to have a high hardness value; otherwise, the frets may embed themselves too easily into the wood. In the case of woodwind instruments, insufficient wood hardness can lead to wear between the metal keys and the wood, potentially resulting in bonding defects. The hardness has been measured using a calibrated *Sauter* Shore-D durometer, ranging from 0 to 100 shore-D with a range accuracy of the unit. The samples were measured in the

165 LR, LT and RT planes, before and after stabilisation. For each sample, 20 hardness  
measurements were taken, five in each of the following cases :

- In the initial wood when distinguishable from the final wood in the RT plane.
- In the final wood when distinguishable from the initial wood in the RT plane.
- In the initial wood, within the same annual growth ring in the LT plane.
- 170 • In the final wood, within the same annual growth ring in the LT plane.

#### 2.2.4 Density

The density has been evaluated as the ratio between the mass measured with KERN scale at  $\pm 0.01$  gram and the volume of the tubes evaluated with a Mitutoyo caliper and diameter gauges, at constant temperature and RH step.

#### 175 2.2.5 Equilibrium Moisture content

The wood equilibrium moisture content  $EMC$  at any given  $RH$  is obtained using the dried mass, denoted as  $m_0$  after heating at  $103^\circ\text{C}$ , using the equation 2. The measurements are made in accordance with the standard D4442-20. Equilibrium moisture content was evaluated when the mass of the sample at a given relative humidity,  $m_{RH}$ , and  $25^\circ\text{C}$  varied by less than 0.05% from its previous measurement value within a  
180 24-hour interval between measurements, as used in (Damay 2014).

$$EMC_{RH} = \frac{m_{RH} - m_0}{m_0} \quad (2)$$

#### 2.2.6 Dimensional stability

The shrinkage and swelling have been evaluated through the volume variations, between two different equilibrium moisture contents, associated with two different relative humidity conditions (30 and 80%). This lower value corresponds to low relative humidity conditions in rooms where instrument may be stored. The higher value also  
185 corresponds to high relative humidity conditions where instruments can be stored without proper relative humidity like in museums. It has to be noted that, in playing conditions for wind instruments, relative humidity inside the instrument can tend  
190 towards greater values, up to, during fairly short periods when it is played, a condensation that can even run down. As this study is a screening of different woods, this condition would be investigated in further study, with most promising wood species.

#### 2.2.7 $\frac{T}{R}$ ratio

In the context of cylindrical instruments, the phenomenon of shrinkage and swelling  
195 leads to out-of-roundness due to the different behaviours of the radial (R) and tangential (T) dimensions in response to humidity variations. Tangential variations between two different humidity levels are about twice as significant as radial variations for most woods. The tangential and radial shrinkage are obtained by measuring the dimensions in the R and T directions. The  $\frac{T}{R}$  ratio, which is usually measured using  
200 standard ISO 13061-13:2016, refers here to the roundness of the tube, and therefore

the potential out-of-roundness of the samples, which is adapted in the particular context of instrument making. Minimal values for this ratio are sought, as they lead to reduced wood out-of-roundness. In this study,  $\frac{T}{R}$  represents the relative variation in tangential diameter over the range of 30-80% RH, divided by the relative variation in radial diameter in the same range. The diameters  $D_T$  and  $D_R$  were obtained by taking cross-sectional measurements with a caliper at five different locations. The value given is based on the average of the five measurements along the longitudinal direction on the radial and tangential directions. 205

### 2.2.8 Air leakage

The air leakage has been measured using a *Musicmedic leak tester* device, provided by *Musicmedic.com*, which is common in musical instruments context to test the leakage of a bore and sealing of the keys. The samples previously tested are immersed in water, with both sides closed. At one side, a pressure is applied. The over-pressure in the bore is equal to 2 kPa and the device controls the leaks. Moreover, the escape of bubbles are verified to check if leaks are present. If a sample presents no leaks the test is considered as passed. 210  
215

### 2.2.9 Weight percent gain

The Weight Percent Gain (WPG) is used to quantify the amount of substance absorbed by the wood. The WPG is expressed in (Zelinka et al. 2022) by:

$$WPG = \frac{m_{\text{stab, dry}} - m_{\text{ini, dry}}}{m_{\text{ini, dry}}} \quad (3)$$

With  $m_{\text{stab, dry}}$  the dry mass of the wood after modification and  $m_{\text{ini, dry}}$  the dry mass of the wood before modification. 220

### 2.2.10 Moisture exclusion efficiency

The Moisture Exclusion Efficiency (MEE) measures the ability of the stabilised wood to exclude moisture compared to its initial state. The moisture exclusion efficiency is given in Zelinka et al. (2022) by: 225

$$MEE = 1 - \frac{EMC_{50\text{stab}}}{EMC_{50\text{ini}}} \quad (4)$$

with  $EMC_{50\text{stab}}$  is the equilibrium moisture content at 50% relative humidity (RH) for the stabilised wood and  $EMC_{50\text{ini}}$  is the equilibrium moisture content at 50% RH for the initial (unmodified) wood. It is corrected for  $WPG > 0$  as:

$$MEE_{\text{corrected}} = 1 - \frac{EMC_{50\text{stab}}}{EMC_{50\text{ini}}} (1 + WPG) \quad (5)$$

### 2.2.11 Anti-swelling efficiency

The Anti-Swelling Efficiency (ASE) evaluates the effectiveness of the treatment in preventing the swelling of the wood due to moisture absorption. It compares the 230

swelling behaviour of modified wood to unmodified wood at a specific equilibrium moisture content. Swelling of stabilised state  $S_{\text{stab,EMC}}$  or initial state  $S_{\text{ini,EMC}}$  wood is defined in [Zelinka et al. \(2022\)](#) by:

$$S_{EMC} = \frac{V_{EMC} - V_d}{V_d} \quad (6)$$

235 With  $V_{EMC}$  is the volume of the wood at a given equilibrium moisture content and  $V_d$  is the dry volume of the wood (initial or stabilised state). The ASE accounts for the bulking effect introduced by the treatment, which can influence the swelling behaviour. It is given by [Zelinka et al. \(2022\)](#):

$$ASE = 1 - \frac{S_{\text{stab,EMC}}}{S_{\text{ini,EMC}}} \quad (7)$$

240 Where  $S_{\text{stab,EMC}}$  is the swelling of the stabilised wood at a given EMC and  $S_{\text{ini,EMC}}$  the swelling of the initial wood at the same EMC.

### 2.2.12 First Eigenfrequency of a Free-Free Beam

For a rectangular cross-section, free conditions Euler-Bernoulli beam of length  $L$ , width  $b$  and thickness  $h$ , the first eigenfrequency is given by:

$$f_1 = \frac{4.73^2}{2\pi} \sqrt{\frac{E_L I}{\rho A L^4}} \quad (8)$$

245 where  $I$  is the moment of inertia and  $A$  the cross-sectional area,  $\rho$  the density,  $L$  the length and  $E$  the Young's modulus in  $L$  direction.

$$I = \frac{bh^3}{12}, \quad A = bh \quad (9)$$

Elastic modulus is obtained by:

$$E_L = \frac{f_1^2 4\pi^2 \rho A L^4}{4.73^4 I} \quad (10)$$

250 This method is increasingly used by makers in their workshop or during dedicated training sessions, as shown in figure 4. The method consists in holding the beam at flexure mode node (22.4% of  $L$ ) and knocking it in the middle using, for example, a piano hammer. The software *Room Eq. Wizard* ([Mulcahy 2014](#)) can be used for the frequency evaluation. Inferences based on the knowledge of the usual properties of woods by [Guitard and El Amri \(1987\)](#); [Viala \(2018\)](#) can help finding the correct frequency. When the ratio between thickness and length increases, the conditions are different than Euler-Bernoulli beam and corrections have been proposed by [Kocatürk and Simsek \(2005\)](#).

**Figure 4:** Measurement examples. Left: first bending mode, blue color corresponds to nodal lines, simulations made with the software Simscale (Gmbh 2024). Practical Workshop made with makers, measurement of the first bending frequency on a wood beam.



### 2.2.13 X-ray tomography

The three most promising species have been imaged before and after stabilisation by X-ray tomography. An *EASYTOM* (RX-SOLUTION, Chavanod, France) equipment was used to scan the samples at the same location before and after stabilisation. The whole samples were scanned at a resolution of  $1 \mu\text{m}$  with a voltage of 60kV and a current of  $87 \mu\text{A}$ . The number of projections was fixed at 1440 over  $360^\circ$  with an exposure time of 400 ms and an average of 5 images in start and stop mode. These parameters lead to a tomography time of 1 hour per specimen. The reconstruction based on the radiographs was performed with *X-act* software to create vertical slices with a filtered back-projection algorithm. The slices were analysed with *VG Studiomax* 2024 software. The volume fraction of the pores was calculated with an algorithm based on gray levels with material and void levels defined on manually selected areas. Once the porosity volume is computed, it is divided by the total volume.

## 3 Results

All numerical results presented in this section are summarised, and detailed statistics and paired tests are provided in the Supplementary Data (Tables 7-10). Figures illustrate representative evolutions for density, hardness, moisture-dependent behaviour, and acoustic loss factor. The results are reported as mean  $\pm$  standard deviation.

### 3.1 Density and hygroscopic response

275 The stabilisation process led to a significant increase in oven-dry and conditioned densities for all temperate species (Fig. 5, Table 3, Tables 7-8). The densification ranged between 20 % and 60 %, depending on species and anatomical structure. The highest post-treatment densities were obtained for *Carpinus betulus*, spalted *Fagus sylvatica*, and *Acer* spp., with average values close to 1000 kg.m<sup>-3</sup>. These results  
280 indicate efficient polymer uptake and retention within the cell lumen and partly within the cell walls.

The weight percent gain differs according to the species (Fig. 6 and Table 9). For *Fraxinus* genus and different stabilisation products, the WPG is comprised between 14 and 23%. For relatively low-density woods, *Sequoia sempervirens*, *Prunus avium* and *Cedrus atlantica*, the WPG is equal to 31, 32 and 59% respectively. Considering  
285 *Olea europaea* and *Robinia pseudoacacia*, there is almost no increase (4%), meaning that these wood are not suitable to gain MMA under the presented method.

The equilibrium moisture content (EMC) at 50% relative humidity decreased markedly after stabilisation, from values of 8–10% in untreated wood to 2–5% in treated samples. The corresponding moisture exclusion efficiency (MEE) (Fig. 6)  
290 ranged from 40% to more than 70%, while the anti-swelling efficiency (ASE) calculated from tangential and radial dimensions showed similar improvements. The reduction in EMC is consistent with polymer occupation of void space and partial occlusion of pathways to hygroscopic hydroxyl sites.

**Figure 5:** Density comparison for initial and stabilised states represented as box plots for species at 50% RH, with mean values and standard deviation, before and after stabilisation.

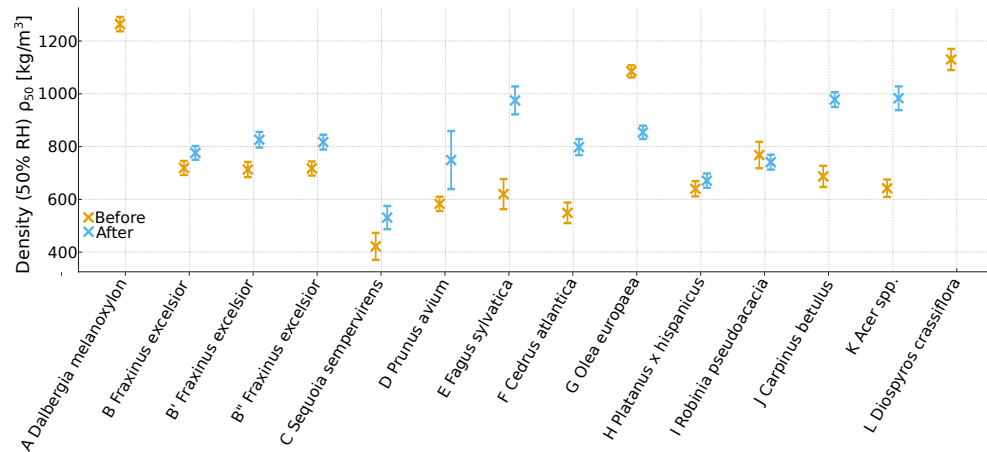


**Table 3:** Relative changes (%) of physical parameters after stabilisation.  $p$ -values estimated from paired  $t$ -tests ( $n = 6$ ) comparing before/after means  $\pm$  standard deviation.

Species	$\rho_{50}$	$\rho_{80}$	$\rho_{30}$	$\Delta D_{T_{30-80}}$	$\Delta D_{R_{30-80}}$	$\frac{T}{R}$
<i>B Fraxinus excelsior</i>	+8 (0.04)	+6.7 (0.05)	+12 (0.02)	-22 (0.19)	-13 (0.2)	-10 (0.33)
<i>B' Fraxinus excelsior</i>	+16 (<0.001)	+16 (<0.001)	+20 (<0.001)	-22 (0.1)	-21 (0.1)	0 (0.9)
<i>B'' Fraxinus excelsior</i>	+14 (0.005)	+13 (0.01)	+18 (0.005)	-18 (0.1)	-22 (0.1)	+10 (0.4)
<i>C Sequoia sempervirens</i>	+26 (0.02)	+26 (0.02)	+32 (0.01)	-22 (0.2)	0 (NS)	-0.1 (NS)
<i>D Prunus avium</i>	+28 (0.01)	+28 (0.01)	+33 (0.01)	-21 (0.2)	-30 (0.1)	+9 (0.44)
<i>E Fagus sylvatica</i>	+57 (<0.001)	+52 (<0.001)	+62 (<0.001)	-25 (0.04)	-82 (<0.001)	-26 (0.02)
<i>F Cedrus atlantica</i>	+45 (<0.001)	+46 (<0.001)	+51 (<0.001)	-34 (0.01)	-52 (0.005)	+36 (0.03)
<i>G Olea europaea</i>	-21 (0.004)	-14 (0.02)	0 (NS)	-76 (<0.001)	-72 (<0.001)	+7 (0.4)
<i>H Platanus x hispanica</i>	+5 (NS)	+20 (0.03)	+8 (0.05)	-36 (0.01)	-45 (0.005)	0 (NS)
<i>I Robinia pseudoacacia</i>	-4 (NS)	0 (NS)	+2 (NS)	-58 (<0.001)	-58 (<0.001)	-4 (NS)
<i>J Carpinus betulus</i>	+42 (<0.001)	+42 (<0.001)	+47 (<0.001)	-33 (0.005)	-35 (0.005)	+21 (0.04)
<i>K Acer spp.</i>	+53 (<0.001)	+55 (<0.001)	+60 (<0.001)	-22 (0.02)	-26 (0.01)	+9 (0.03)

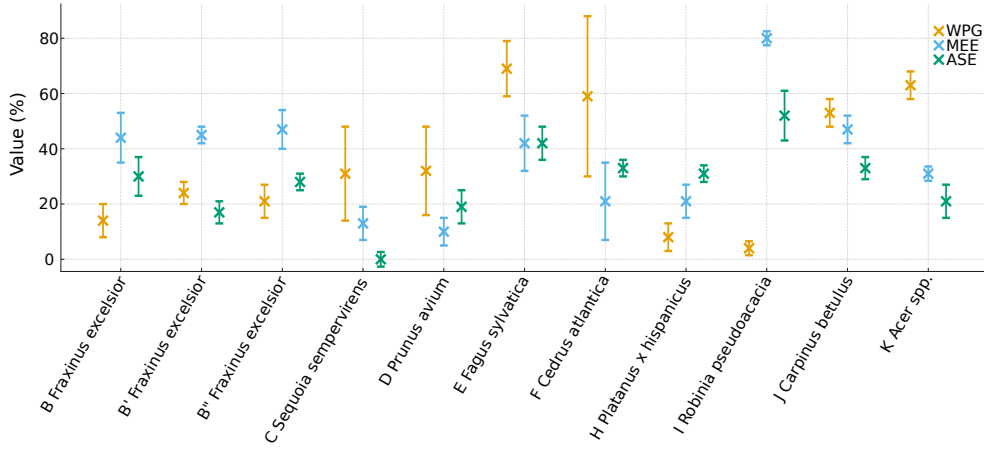


**Figure 6:** Boxplots of mean and standard deviation for WPG, MEE and ASE

Dimensional variations between 30 % and 80 % relative humidity decreased after stabilisation for all tested woods (Tables 7-8) and Fig. 7. The reduction was more pronounced in the tangential direction for most species. For the best-performing species the dimensional changes can be lower than 2% in the R direction and close to 3% in the T direction. The ratio of tangential to radial deformation ( $T/R$ ) reported in table 8 remained between 1.5 and 2.5 depending on species, values comparable to those of *Dalbergia melanoxylon* and without significant changes due to stabilisation.

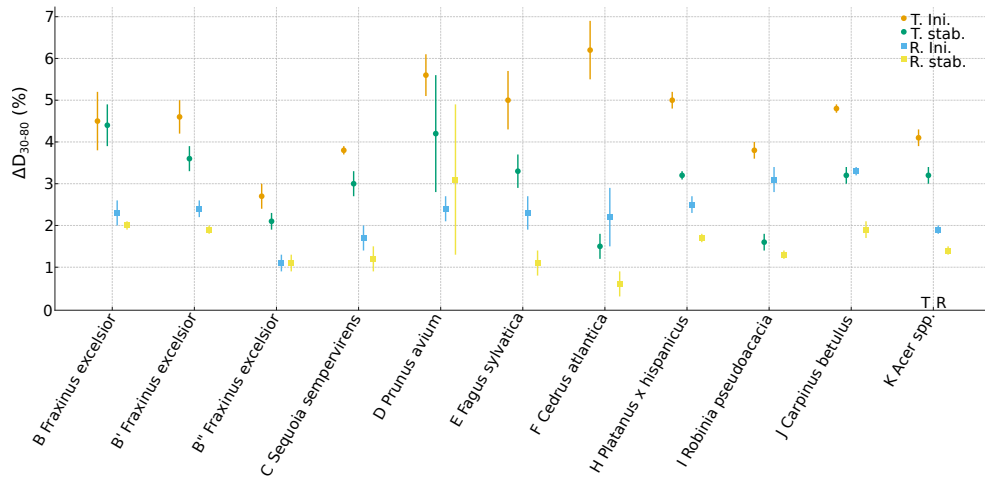
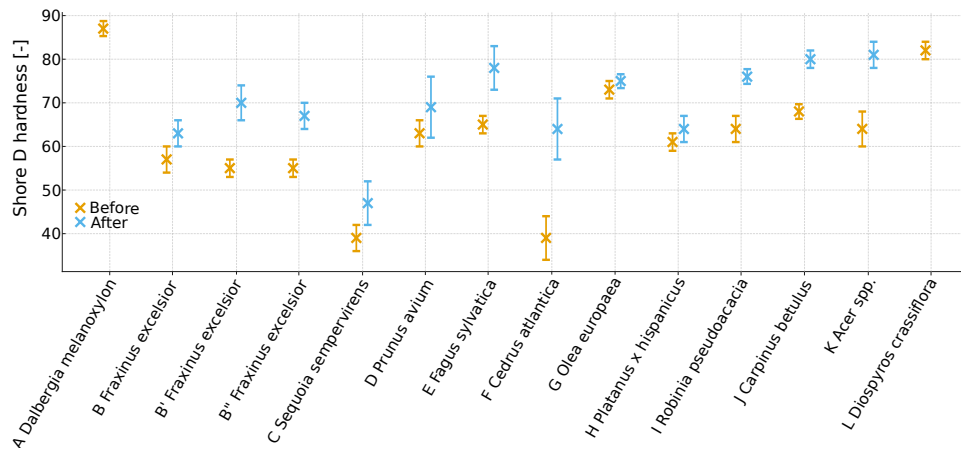


**Figure 7:** Boxplot Mean and standard deviation for Delta T and Delta R, Orange: tangential direction , before stabilisation, green: after stabilisation, tangential direction. Blue : radial direction before stabilisation, yellow: radial, after stabilisation

### 3.2 Hardness

The Shore-D hardness increased systematically after stabilisation (Figure 8, Table 10). The mean hardness of stabilised temperate woods ranged from 72 to 82, compared with 60 to 70 for the untreated state. The highest values were obtained for *Acer* spp. ( $81 \pm 3$ ) and *Carpinus betulus* ( $80 \pm 2$ ). These values approach the reference *Diospyros crassiflora* ( $82 \pm 2$ ) but remain below *Dalbergia melanoxylon* ( $87 \pm 1$ ).

**Figure 8:** Shore-D hardness of tested species before and after (bottom) stabilisation, measured at 50% RH.



### 3.3 Acoustic loss factor and airtightness

The acoustic loss factor ( $\eta$ ), derived from impedance measurements on cylindrical tubes is given in (Figure 9) and Table 4. There is no clear reduction in  $\eta$ , indicating improved acoustic efficiency through lower visco-thermal losses. For the most promising temperate species, *Carpinus betulus* J, *Acer spp.* K, *F. sylvatica* E,  $\eta$  values of 2.3–2.7 % were obtained, approaching, yet higher than, the reference *Dalbergia melanoxydon* (1.8 %) for each relative humidity condition. These species showed the highest values of some parameters (WPG, density, hardness) and deserved further investigations. Leak tests confirmed satisfactory airtightness for most species, except *Prunus avium* and *Cedrus atlantica*, whose higher porosity limited polymer efficiency.

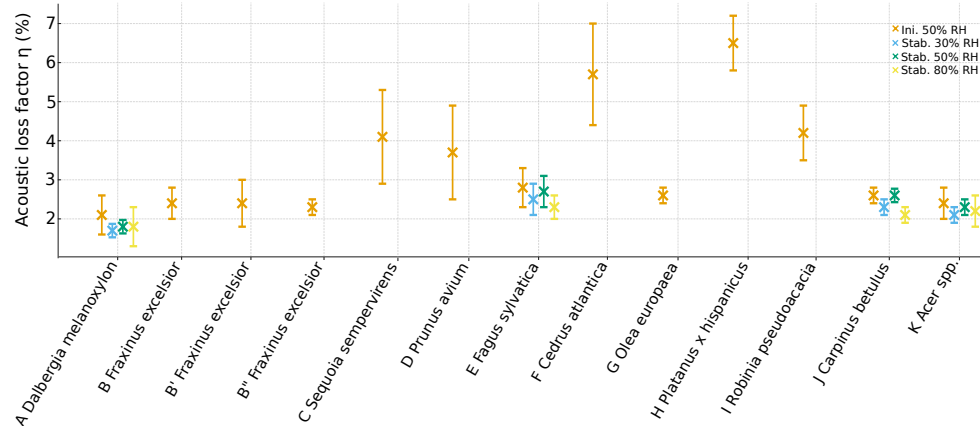


**Figure 9:** Acoustic loss factors (mean and standard deviation) of the air column for all the species at 50% relative humidity, and for different RH for selected species.

**Table 4:** Average $\pm$ standard deviation of acoustic loss factor of the tubes before stabilisation at 50%, and after stabilisation for selected species for 30 and 80% RH. The reference for the relative difference is the loss factor at 50% RH. The samples are with rough bore, without linseed oil or polishing. Results of the permeability tests are given, performed using *Musimedic leak tester*.

Species	$\eta_{50\%}$ ini. [%]	$\eta_{30\%}$ aft. [%]	$\eta_{50\%}$ aft. [%]	$\eta_{80\%}$ aft. [%]	Air tightness [-]
<i>A Dalbergia melanoxylon</i>	2.1 $\pm$ 0.5	1.7 $\pm$ 0.1	1.8 $\pm$ 0.1	1.8 $\pm$ 0.5	Passed
<i>B Fraxinus excelsior</i>	2.4 $\pm$ 0.4	-	-	-	Passed
<i>B' Fraxinus excelsior</i>	2.4 $\pm$ 0.6	-	-	-	Passed
<i>B'' Fraxinus excelsior</i>	2.3 $\pm$ 0.2	-	-	-	Passed
<i>C Sequoia sempervirens</i>	4.1 $\pm$ 1.2	-	-	-	Passed
<i>D Prunus avium</i>	3.7 $\pm$ 1.2	-	-	-	Failed
<i>E Fagus sylvatica</i>	2.8 $\pm$ 0.5	2.5 $\pm$ 0.4	2.7 $\pm$ 0.4	2.3 $\pm$ 0.3	Passed
<i>F Cedrus atlantica</i>	5.7 $\pm$ 1.3	-	-	-	Failed
<i>G Olea europaea</i>	2.6 $\pm$ 0.2	-	-	-	Passed
<i>H Platanus x hispanica</i>	6.5 $\pm$ 0.7	-	-	-	Passed
<i>I Robinia pseudoacacia</i>	4.2 $\pm$ 0.70	-	-	-	Passed
<i>J Carpinus betulus</i>	2.6 $\pm$ 0.2	2.3 $\pm$ 0.2	2.6 $\pm$ 0.1	2.1 $\pm$ 0.2	Passed
<i>K Acer spp.</i>	2.4 $\pm$ 0.4	2.1 $\pm$ 0.2	2.3 $\pm$ 0.2	2.2 $\pm$ 0.4	Passed

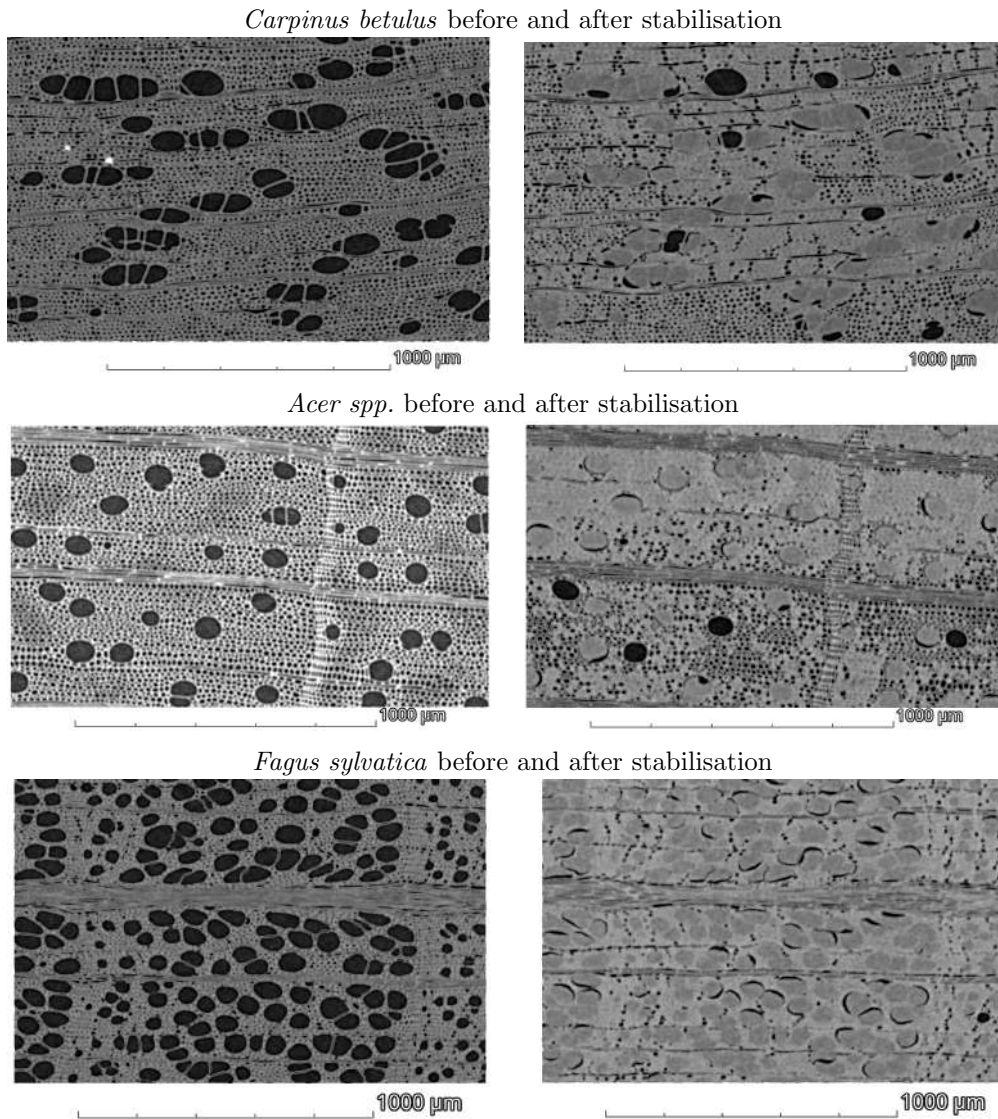
### 3.4 Microtomography and porosity reduction

X-ray microtomography of the most promising species, *Carpinus betulus* J, *Acer spp.* K and *Fagus sylvatica*, revealed significant reductions in open porosity following stabilisation (Figure. 10, Table 5). The fraction of open vessels and ray lumina decreased by 60–85 %, depending on species. Polymer filling was homogeneous at the submillimetric scale, although local heterogeneities were observed. Residual shrinkage gaps of a few micrometres were occasionally observed at vessel walls, consistent with polymerisation shrinkage of MMA. without forming a proper bond with the cell walls. These observations confirm that the major physical changes result from lumen (vessels and fibres) filling.

**Table 5:** Porosity level and relative variation before and after impregnation and polymerisation of MMA, obtained by tomography.

Species	$\%V_{poro.}$ ini. [-]	$\%V_{poro.}$ stab. [-]
<i>A Dalbergia melanoxylon</i>	10	-
<i>E Fagus sylvatica</i>	55	15 (-72%)
<i>J Carpinus betulus stabilised</i>	40	15 (-62%)
<i>K Acer sp.</i>	35	15 (-57%)
<i>L Diospyros crassiflora</i>	15	-

**Figure 10:** Tomographic imaging of: top, *Carpinus Betulus*; middle; *Acer* spp.: bottom: *Fagus sylvatica*; Before (left) and after (right) stabilisation at the same location of the sample



### 3.5 Elastic behaviour for fingerboard application

The longitudinal modulus of elasticity ( $E_L$ ) of stabilised *Carpinus betulus*, presented in Table 6, reached values statistically comparable to those of *Diospyros crassiflora*, with a slightly lower density. This mechanical equivalence, combined with enhanced

330

hardness and reduced hygroscopicity, highlights the potential of stabilised hornbeam for fingerboard applications.

**Table 6:** Average±standard deviation of density and elastic modulus of woods considered for fingerboards, based on 15 samples of *Diospyros crassiflora* and stabilised hornbeam *Carpinus betulus*. (*p-value*) for the comparison with *Diospyros crassiflora*.

Species	Density [ $\frac{kg}{m^3}$ ]	Longitudinal modulus $E_L$ [GPa]
<i>Carpinus betulus</i> <i>Jini</i>	770±50 (<0.001)	14.1±1.1 (<0.001)
<i>Carpinus betulus</i> <i>Jstab</i>	1080±20 (<0.001)	19.8±0.9 (<0.3 )
<i>Diospyros crassiflora</i> <i>L</i>	1130±40	18.8±3.3

## 4 Discussion

### 335 4.1 Structure–property relationships

The correlation between weight percent gain (WPG), porosity reduction, and physical property enhancement supports a mechanism of lumen filling. Microtomographic evidence confirms that the reduction in open porosity directly corresponds to improvements in hardness and moisture stability. The effectiveness of stabilisation depends  
340 strongly on anatomical features: diffuse-porous woods such as *Carpinus* and *Acer* exhibit homogeneous polymer distribution, whereas ring-porous, and wood with tyloses such as *Robinia pseudoacacia* or extractive-rich such as *Olea europaea* show local inhibition of impregnation.

### 4.2 Hygroscopic and dimensional stability

The reduction in EMC and dimensional change is consistent with prior reports on MMA-treated poplar and pine (Ding et al. 2012; Acosta et al. 2020; Priadi et al. 2020). The filling of lumen and the partial blockade of pathway to hydroxyl groups by polymer chains limit swelling of the cell wall. The remaining anisotropy ( $T/R$ ) is governed by the intrinsic anatomical structure, which stabilisation cannot entirely  
350 remove. Nevertheless, the absolute reduction in dimensional variation is interesting for maintaining bore geometry for woodwind instruments.

### 4.3 Hardness and mechanical performance

The increases in Shore-D hardness are consistent with earlier observations for MMA-impregnated hardwoods (Hadi et al. 2019; Kim et al. 2020). *Cedrus atlantica*, in particular, experienced a significant increase, from 39±5 to 64±7. Generally, species  
355 with the highest initial hardness among the hardwoods also exhibit the highest values after stabilisation. However, *Olea europaea*, *Robinia pseudoacacia*, and *Prunus avium* did not witness the same degree of hardness increase as the three selected species, likely due to a resin impregnation failure for these species where density increase and

WPG is particularly low. Except for these three species, the stabilisation process raised the average Shore-D hardness of the hardwoods to similar levels. Also, some species, such as the softwoods, had initial values very low to meet the desired threshold. The mechanical stiffening originates from the higher local modulus of PMMA compared with the lignocellulosic matrix and from the physical reinforcement of voids, avoiding collapse of cells. From a functional standpoint, the obtained hardness values increase capability of wear resistance for key seating and fingerboard applications.

#### 4.4 Acoustic loss factor and relevance to instrument performance

There was no substantial changes in acoustic loss factors. For the three selected species, the difference compared with *Dalbergia melanoxylon* can be attributed to remaining micro-roughness, partial filling, MMA polymerisation shrinkage and the absence of final polishing or oiling steps, which typically further reduce damping in finished instruments. In this respect, the stabilised temperate woods reach, before finishing steps, values close yet higher than *Dalbergia melanoxylon*.

#### 4.5 Wood Structure Results

##### 4.5.1 Softwoods

The structure of softwoods, consisting mainly of cells with diameters around 10  $\mu\text{m}$  according to studies by Pittermann and Sperry (2006) (with an average value of  $11.0 \pm 1.1 \mu\text{m}$  for *Pinus contorta* and  $8.4 \pm 0.5 \mu\text{m}$  for *Juniperus scopulorum*), leads to thin walls and large lumens in the earlywood. In most cases, earlywood constitutes a large fraction of the total wood (Polge 1966), which impacts wood density, explaining why softwoods typically have densities below  $500 \frac{\text{kg}}{\text{m}^3}$  (although larch can reach higher values). The high porosity of these woods could explain both the high amount of MMA impregnation, likely concentrated mostly in the lumens, but also the failure to reach a density close to that of *Dalbergia melanoxylon*. This porosity could also contribute to insufficient Shore-D hardness and excessively high acoustic loss factors due to significant visco-thermal losses associated with porosity and rugosity.

##### 4.5.2 Temperate Hardwoods

Understanding the behaviour of temperate hardwoods is more complex, primarily because the results vary significantly with species. As expected, hardwoods have higher densities than softwoods, as seen in the  $\rho_{50}$  measurements during the experimental campaign. For many tropical hardwoods, seasonality is less pronounced than in temperate climates, which can lead to greater wood homogeneity, which is in favour of the values achieved for the analysed descriptors for *Dalbergia melanoxylon*. Another significant factor is the high proportion of extractive in *Dalbergia melanoxylon* (around 20% of the mass), which significantly increases wood density. The temperate hardwoods tested have a lower proportion of extractives. Nevertheless, there was a significant mass loss in *Olea europaea* samples during drying just before stabilisation. This loss appears related to the removal of a portion of wood extractive, as the wood density did not return to its initial value after a new adsorption phase up to 50% RH and

400 before stabilisation. It is possible that the high proportion of extractive hindered the  
penetration of MMA into the wood, which was already very dense ( $1085 \pm 23 \text{ kg/m}^3$ ).  
For *Robinia pseudoacacia*, it is also likely that the high presence of tyloses of this  
specie, as discussed in Darshani et al. (2025) plays a significant role without a signifi-  
cant amount of extractives. For the hardwoods that achieved values close to *Dalbergia*  
405 *melanoxylon* after impregnation, the exact process remains unclear. MMA is generally  
considered to be mainly concentrated in lumens. According to Zelinka et al. (2022),  
the presence of water acting as a solvent is useful for MMA diffusion into the cell  
walls. However, guidelines for the used resins suggests oven heating for water evapo-  
ration. This step may have hindered MMA diffusion. Wood porosity, vessel size and  
410 type could play an important role in wood impregnability. In the case of spalted beech,  
which showed promising results, the spalted characteristics increased wood porosity  
due to fungal activity, which degraded some wood components, and might lead to a  
high variability of the response. Similarly, to understand this phenomenon,  $\mu$ CT scan,  
as presented, yield insights on the MMA shrinkage and uneven distribution, as several  
415 vessels remain empty although surrounded by filled fibres and vessels.

#### 4.6 Limitations of the current state of knowledge

The present results extend beyond the explanatory capacity of existing models and  
datasets on polymer-impregnated wood. Earlier studies of MMA treatments have pri-  
marily addressed improvements in density, hardness, or dimensional stability, like Ding  
420 et al. (2012); Acosta et al. (2020); Hadi et al. (2019); Priadi et al. (2020); Kim et al.  
(2020), often under static conditions and without correlation to acoustic or microstruc-  
tural descriptors. Comprehensive analyses linking micro-scale impregnation patterns  
to macro-scale acoustic losses remain scarce. Although microtomography has been ap-  
plied to assess porosity in wood by Trtik et al. (2007); Sedighi Gilani et al. (2014);  
425 Bucur (2006), its use to interpret visco-thermal damping mechanisms or impedance-  
derived loss factors has not yet been established. Existing physical models of acoustic  
dissipation in porous wood ducts, by Keefe (1984); Nederveen (1998); Chaigne and  
Kergomard (2016) describe viscothermal and wall losses for ideal geometries, but they  
do not account for local polymer distribution, anatomical anisotropy, or hygroscopic  
430 changes introduced by stabilisation. Likewise, empirical correlations between weight  
percent gain and dimensional stability proposed by Wu et al. (2017); Sandberg et al.  
(2017) are insufficient to predict acoustic damping, which depends on multi-scale  
interactions between porosity, polymer stiffness, and moisture content.

Consequently, the current state of the art does not provide an integrated frame-  
435 work capable of predicting the combined physical and acoustic response of stabilised  
wood. The present work addresses this gap by jointly measuring moisture-dependent  
dimensional behaviour, hardness, and impedance-derived acoustic losses, and by quan-  
tifying pore filling through X-ray tomography. This combined methodology enables  
a mechanistic description of stabilisation effects that extends beyond the scope of  
440 existing studies.

## 4.7 Implications for sustainable instrument manufacturing

From a practical perspective, the stabilisation of temperate species such as *Carpinus betulus*, spalted *Fagus sylvatica*, and *Acer spp.* offers a viable path toward reducing dependence on endangered tropical timbers. The cross-species comparison under an identical craft-compatible MMA protocol shows that these species jointly satisfy the most stringent set of instrument-oriented criteria (density near  $1\text{ g cm}^{-3}$ , low EMC, high Shore-D, low bore-loss  $\eta$ , acceptable  $T/R$ , and airtightness). Their local availability and process compatibility make them promising candidates for sustainable instrument making. Prototypes have already been made using stabilised spalted wood, as shown on figure 11. Additional work integrating environmental life-cycle assessment and musician feedback would be necessary before large-scale implementation. As practical guidances, for woodwinds, *Carpinus betulus* and *Acer spp.* are the strongest candidates. For fingerboards, stabilised *Carpinus betulus* achieves  $E_L$  comparable to *Diospyros* with slightly lower density. It has to be pointed out that dyes/stains can be applied for aesthetics and finishes reduce direct skin-wood contact.



**Figure 11:** Prototypes realised with stabilised spalted wood, following the present study. Violin made by the authors with stabilised wood chinrest, tailpiece and finger-board, based on an unvarnished body. Irish flute made by a student of ITEM (D. ROGEAU).

The present study used a single impregnation protocol under vacuum without over-pressure to ensure reproducibility and craft compatibility. The influence of viscosity, vacuum duration, or pressure cycles on impregnation depth was not investigated and may further enhance performance. Curing shrinkage occasionally generated small voids visible in tomography, which could be mitigated by optimising polymerisation kinetics. The acoustic loss factor was evaluated on straight, unpolished tubes; future studies should include instrument prototypes incorporating tone holes, keys, and realistic bore finishing to quantify the effective acoustic benefit under playing conditions.

## 5 Conclusion and perspectives

465 The purpose of this study was to propose approaches to handle the scarcity of instrumental wood resources, coupled with stricter import regulations, especially for tropical species like *Dalbergia melanoxylon* and *Diospyros crassiflora*. The two main objectives were to identify substitute wood species from temperate regions, following a short supply chain logic and less pressure on vulnerable ecosystems. Three potential alternative wood species were identified in this study: *Carpinus betulus*, *Fagus sylvatica* (at least in spalted form), and *Acer spp.*. Stabilisation through impregnation with methyl methacrylate allowed for obtaining characteristics closer to those of *Dalbergia melanoxylon* or *Diospyros crassiflora* for main descriptors associated with woodwind instruments and fingerboards production, though without reaching them. 470  
475 This research contributes to the development of sustainable and acoustically appropriate materials for instruments where specific mechanical properties are relevant. To further approach the properties of tropical reference woods, future studies may investigate mechanical densification, thermal treatment, or chemical polymer bonding.

**Acknowledgements.** The authors acknowledge the French government through the project *BLIV: Bois Locaux pour Instrument à Vent* under the *France 2030, Alternatives vertes* plan. The authors acknowledge the MIFHySTO platform of the FEMTO-ST institute for providing access to the X-ray microtomographer. Stéphane NEIDHARDT, graphic designer has created the images of Figure 1. Damien ROGEAU has made the Irish flute shown in Figure 11.

## 485 References

- Ablitzer, F.: Peak-picking identification technique for modal expansion of input impedance of brass instruments. *Acta Acustica* **5** (2021) <https://doi.org/10.1051/aacus/2021046>
- 490 Alkadri, A., Jullien, D., Arnould, O., Rosenkrantz, E., Langbour, P., Hovasse, L., Gril, J.: Hygromechanical properties of grenadilla wood (*Dalbergia melanoxylon*). *Wood Science and Technology* **54**(5), 1269–1297 (2020) <https://doi.org/10.1007/s00226-020-01215-z>
- 495 Acosta, A.P., Labidi, J., Schulz, H.R., Gallio, E., Barbosa, K.T., Beltrame, R., de Avila Delucis, R., Gatto, D.A.: Thermochemical and mechanical properties of pine wood treated by in situ polymerization of methyl methacrylate (mma). *Forests* **11**(7), 1–10 (2020) <https://doi.org/10.3390/F11070768>
- 500 Boutin, H., Le Conte, S., Vaiedelich, S., Fabre, B., Le Carrou, J.-L.: Acoustic dissipation in wooden pipes of different species used in wind instrument making: An experimental study. *The Journal of the Acoustical Society of America* **141**(4), 2840–2848 (2017) <https://doi.org/10.1121/1.4981119>
- Bucur, V.: *Acoustics of Wood*, 2nd edn. Springer, ??? (2006). <https://doi.org/10.1007/3-540-30594-7>

- Chaigne, A., Kergomard, J.: Acoustics of Musical Instruments. Springer, ??? (2016). <https://doi.org/10.1007/978-1-4939-3679-3>
- Calvano, S., Negro, F., Ruffinatto, F., Zanuttini-Frank, D., Zanuttini, R.: Use and sustainability of wood in acoustic guitars: An overview based on the global market. *Heliyon* **9**(4), 15218 (2023) <https://doi.org/10.1016/j.heliyon.2023.e15218> 505
- Convention On International Trade In Endangered Species Of Wild Fauna And Flora (CITES): Proposal for amendment of Appendix I or II for CITES CoP17: Inclusion of the genus *Dalbergia* in CITES Appendix II. Seventeenth meeting of the Conference of the Parties, Johannesburg, South Africa (2016). <https://cites.org/eng/cop/17/prop/index.php> 510
- Damay, J.: Développement de nouveaux traitements du bois basés sur le procédé d'imprégnation axiale. Thesis, Université de Lorraine, Vandœuvre-lès-Nancy (2014). <https://doi.org/10.2737/FPL-GTR-50> 515
- Ding, W.D., Koubaa, A., Chaala, A., Belem, T., Krause, C.: Relationship between wood porosity, wood density and methyl methacrylate impregnation rate. *Wood Material Science and Engineering* **3**(1-2), 62–70 (2008) <https://doi.org/10.1080/17480270802607947>
- Ding, W.-D., Koubaa, A., Chaala, A.: Dimensional stability of methyl methacrylate hardened hybrid poplar wood. *BioResources* **7**(1), 504–520 (2012) 520
- Dalmont, J.-P., Le Roux, J.C.: A new impedance sensor for wind instruments. *The journal of the Acoustical Society of America* **123**(5\_Supplement), 3014 (2008)
- Darshani, P., Sharma, S., Harisha, C.R., Patel, B., Negi, R., Yadav, A.N.: Tylosis formation and micro evaluation of three different heartwood of Devadaru, Sarala and Vijaysar: a scientific study. *Proceedings of the Indian National Science Academy (September)* (2025) <https://doi.org/10.1007/s43538-025-00497-w> 525
- Esteves, B.: Effect of heat treatment on shore-D hardness of some wood species. *BioResources* **16**, 1482–1495 (2021) <https://doi.org/10.15376/biores.16.1.1482-1495>
- Guitard, D., El Amri, F.: Modèles prévisionnels de comportement élastique tridimensionnel pour les bois feuillus et les bois résineux (Predictive models of three-dimensional elastic behaviour for hardwoods and softwoods). *Annales des sciences forestières* **44**(3), 335–358 (1987) 530
- Gmbh, S.: SimScale - Cloud-Based Engineering Simulation Platform (2024). <https://www.simscale.com> 535
- Gibiat, V., Selmer, J., Halary, J.-L.: Wood-treatment method comprising in situ polymerization under electromagnetic radiation (2007)

- Hill, C.A.S.: Wood Modification : Chemical, Thermal and Other Processes. Wiley, New Jersey (2006)
- 540 Hadi, Y.S., Massijaya, M.Y., Zaini, L.H., Pari, R.: Physical and mechanical properties of mma-wood (mma-impregnated wood from three fast-growing tropical tree species). *Journal of the Korean Wood Science and Technology* **47**(3), 324–335 (2019) <https://doi.org/10.5658/WOOD.2019.47.3.324>
- 545 Hu, Y., Wu, Y., Chen, X., Yuan, L., Tian, L., Wang, J.: Methyl methacrylate in wood polymerisation in bulk prepares the method for vitrifying timber (2013)
- ITEMM, CSFI: Guides Des Bonnes Pratiques, Bois et Cuivres, Instruments à Vent (Practical guide for brass and woodwinds instruments). Technical report, Institut Technologique Européen des Métiers de la Musique (2020)
- ITEMM, CSFI: Good Practice Guide, Bowed String Instruments (2021)
- 550 Jones, D., Sandberg, D.: A Review of Wood Modification Globally – Updated Findings from COST FP1407. *Interdisciplinary Perspectives on the Built Environment* **1**(December 2020) (2020) <https://doi.org/10.37947/ipbe.2020.vol1.1>
- 555 Keefe, D.H.: Acoustical wave propagation in cylindrical ducts: Transmission-line parameter approximations and boundary layer effects. *Journal of the Acoustical Society of America* **75**(1), 58–62 (1984)
- Kim, I., Karlsson, O., Myronycheva, O., Jones, D., Sandberg, D.: Methacrylic resin for protection of wood from degradation and stabilisation. *BioResources* **15**(3), 7018–7033 (2020). DIVA Portal thesis/technical report
- 560 Kocatürk, T., Simsek, M.: Free Vibration Analysis Of Timoshenko Beams Under Various Boundary Conditions. *Journal of Engineering and Natural Sciences* (0212), 30–44 (2005)
- Mulcahy, J.: Room EQ Wizard: Room Acoustics Software. Rev (2014)
- Nederveen, C.J.: *Acoustical Aspects of Woodwind Instruments*, 2nd edn. Northern Illinois University Press, DeKalb, Illinois (1998)
- 565 Priadi, T., Orfian, G., Cahyono, T.D., Iswanto, A.H.: Dimensional Stability, Color Change, and Durability of Boron-MMA Treated Red Jabon (*Antocephalus macrophyllus*) *Wood* **48**(3), 315–325 (2020)
- 570 Polge, H.: Établissement des courbes de variation de la densité du bois par exploration densitométrique de radiographies d'échantillons prélevés à la tarière sur des arbres vivants : applications dans les domaines Technologique et Physiologique (Establishment of wood density variation curves by densitometric analysis of radiographs of increment-core samples taken from living trees: technological and

- physiological applications). *Annales des Sciences Forestières* **23**(1), 1–206 (1966) <https://doi.org/10.1051/forest/19660101>
- Pittermann, J., Sperry, J.S.: Analysis of Freeze-Thaw Embolism in Conifers. The Interaction between Cavitation Pressure and Tracheid Size. *Plant Physiology* **140**(1), 374–382 (2006) <https://doi.org/10.1104/pp.105.067900> 575
- Stolf, D.O., Bertolini, M.d.S., Christoforo, A.L., Panzera, T.H., Ribeiro Filho, S.L.M., Lahr, F.A.R.: *Pinus caribaea* var. *hondurensis* Wood Impregnated with Methyl Methacrylate. *Journal of Materials in Civil Engineering* **29**(6), 1–6 (2017) [https://doi.org/10.1061/\(asce\)mt.1943-5533.0001830](https://doi.org/10.1061/(asce)mt.1943-5533.0001830) 580
- Sedighi Gilani, M., Boone, M.N., Mader, K., Schwarze, F.W.M.R.: Synchrotron X-ray micro-tomography imaging and analysis of wood degraded by *Physisporinus vitreus* and *Xylaria longipes*. *Journal of Structural Biology* **187**(2), 149–157 (2014) <https://doi.org/10.1016/j.jsb.2014.06.003> 585
- Sandberg, D., Haller, J., Navi, A.: Thermo-hydro and thermo-hydro-mechanical wood processing: an opportunity for future environmentally friendly wood products. *Wood Material Science & Engineering* **12**(1), 76–85 (2017) <https://doi.org/10.1080/17480272.2016.1266924>
- Schatz, G.E., Lowry, P.P.I., Onana, J.-M., Stévant, T., Deblauwe, V.: *Diospyros crassiflora*. The IUCN Red List of Threatened Species 2019: e.T33048A2831968. Accessed on 01 December 2025 (2019). <https://doi.org/10.2305/IUCN.UK.2019-1.RLTS.T33048A2831968.en> . <https://dx.doi.org/10.2305/IUCN.UK.2019-1.RLTS.T33048A2831968.en> 590
- Trtik, P., Dual, J., Keunecke, D., Mannes, D., Niemz, P., Stähli, P., Kaestner, A., Groso, A., Stampanoni, M.: 3d imaging of microstructure of spruce wood. *Journal of structural biology* **159**(1), 46–55 (2007) 595
- TurnTex, LLC: Cactus Juice Stabilizing Resin: Technical Data Sheet. TurnTex, LLC, Belton, TX, USA (2024). TurnTex, LLC. Product technical data sheet. <https://www.turntex.com/cactus-juice-stabilizing-resin> 600
- Viala, R.: Towards a model-based decision support tool for stringed musical instrument making. PhD thesis, Université Bourgogne Franche-comté (2018). <https://hal.archives-ouvertes.fr/tel-02877895>
- Wu, G., Shah, D.U., Janeček, E.-R., Burridge, H.C., Reynolds, T.P., Fleming, P.H., Linden, P., Ramage, M.H., Scherman, O.A.: Predicting the pore-filling ratio in lumen-impregnated wood. *Wood Science and Technology* **51**(6), 1277–1290 (2017) 605
- Wolfe, J., Smith, J., Tann, J., Fletcher, N.H.: Acoustic impedance spectra of classical and modern flutes. *Journal of Sound and Vibration* **243**(1), 127–144 (2001) <https://doi.org/10.1006/jsvi.2000.3346>

- 610 Yang, L., Xu, W.Z., Zomaya, D., Charpentier, P.A.: Softwood impregnation by mma  
monomer using supercritical co<sub>2</sub>. *The Journal of Supercritical Fluids* **189**, 105712  
(2022)
- Zelinka, S.L., Altgen, M., Emmerich, L., Guigo, N., Keplinger, T., Kymäläinen,  
615 M., Thybring, E.E., Thygesen, L.G.: Review of Wood Modification and Wood  
Functionalization Technologies. *Forests* **13**(7), 1004 (2022) [https://doi.org/10.3390/  
f13071004](https://doi.org/10.3390/f13071004)

## Declarations

- Funding
  - The study was funded by the French state through the program *FRANCE*  
620 *2030*, with the project *BLIV Bois locaux Instruments à Vent*.
- Conflict of interest/Competing interests
  - The authors declare having no conflict of interest
- Ethics approval and consent to participate
  - Not applicable
- 625 • Consent for publication
  - Not applicable
- Data availability
  - Available upon request
- Materials availability
  - 630 – Available upon request
- Code availability
  - Not applicable
- Author contribution
  - 635 – RV and JC obtained funding, NM and RV conducted experimental campaigns  
and provided study reports. RV, NM and JC wrote the paper.

## A Supplementary data

**Table 7:** Table of raw physical data averages by wood species measured before stabilisation. Average  $\pm$  standard deviation. For the sake of readability, average values are provided rather than values for each sample.  $\rho_i$  give the density in  $\frac{kg}{m^3}$  at  $i\%$  RH.  $\Delta_{DT_{30-80}}$  and  $\Delta_{DR_{30-80}}$  and represent the relative change in tangential and radial diameters between 30 and 80% RH respectively.  $\frac{T}{R}$  give ratio between 30 and 80% RH.

Species	$\rho_{50}$ [ $\frac{kg}{m^3}$ ]	$\rho_{80}$ [ $\frac{kg}{m^3}$ ]	$\rho_{30}$ [ $\frac{kg}{m^3}$ ]	$\rho_0$ [ $\frac{kg}{m^3}$ ]	$\Delta_{DT_{30-80}}$ [%]	$\Delta_{DR_{30-80}}$ [%]	$\frac{T}{R}$ [-]
<i>A Dalbergia Melanoxylon</i>	1264 $\pm$ 16	1244 $\pm$ 17	1196 $\pm$ 17	1190 $\pm$ 17	0.2 $\pm$ 0.2	0.2 $\pm$ 0.2	2.0 $\pm$ 1.7
<i>B Fraxinus excelsior</i>	719 $\pm$ 21	734 $\pm$ 17	698 $\pm$ 21	685 $\pm$ 21	4.5 $\pm$ 0.7	2.3 $\pm$ 0.3	2.0 $\pm$ 0.5
<i>B' Fraxinus excelsior</i>	713 $\pm$ 12	727 $\pm$ 11	695 $\pm$ 13	678 $\pm$ 11	4.6 $\pm$ 0.4	2.4 $\pm$ 0.2	1.9 $\pm$ 0.2
<i>B'' Fraxinus excelsior</i>	717 $\pm$ 10	736 $\pm$ 6	698 $\pm$ 10	682 $\pm$ 11	4.5 $\pm$ 0.4	2.2 $\pm$ 0.9	1.9 $\pm$ 0.3
<i>C Sequoia sempervirens</i>	422 $\pm$ 51	429 $\pm$ 5	398 $\pm$ 46	383 $\pm$ 45	2.7 $\pm$ 0.3	1.1 $\pm$ 0.2	2.3 $\pm$ 0.4
<i>D Prunus avium</i>	583 $\pm$ 27	594 $\pm$ 3	563 $\pm$ 28	549 $\pm$ 27	3.8 $\pm$ 0.1	1.7 $\pm$ 0.3	2.3 $\pm$ 0.4
<i>E Fagus sylvatica</i>	620 $\pm$ 57	632 $\pm$ 6	605 $\pm$ 56	591 $\pm$ 56	5.6 $\pm$ 0.5	2.4 $\pm$ 0.3	2.3 $\pm$ 0.1
<i>F Cedrus atlantica</i>	549 $\pm$ 39	556 $\pm$ 127	530 $\pm$ 125	516 $\pm$ 124	5.0 $\pm$ 0.7	2.3 $\pm$ 0.4	2.2 $\pm$ 0.6
<i>G Olea europaea</i>	1085 $\pm$ 23	1034 $\pm$ 19	874 $\pm$ 25	869 $\pm$ 26	6.2 $\pm$ 0.7	2.2 $\pm$ 0.7	2.7 $\pm$ 0.4
<i>H Platanus x hispanica</i>	640 $\pm$ 29	648 $\pm$ 26	621 $\pm$ 25	609 $\pm$ 26	5.0 $\pm$ 0.2	2.5 $\pm$ 0.2	2.0 $\pm$ 0.1
<i>I Robinia pseudoacacia</i>	768 $\pm$ 50	776 $\pm$ 7	741 $\pm$ 6	740 $\pm$ 16	3.8 $\pm$ 0.2	3.1 $\pm$ 0.3	1.25 $\pm$ 0.1
<i>J Carpinus betulus</i>	687 $\pm$ 40	698 $\pm$ 5	671 $\pm$ 6	655 $\pm$ 6	4.8 $\pm$ 0.1	3.3 $\pm$ 0.1	1.4 $\pm$ 0.05
<i>K Acer</i>	642 $\pm$ 33	636 $\pm$ 35	619 $\pm$ 35	606 $\pm$ 35	4.1 $\pm$ 0.2	1.9 $\pm$ 0.1	2.1 $\pm$ 0.2
<i>L Diospyros crassiflora</i>	1130 $\pm$ 40	-	-	-	-	-	-

**Table 8:** Table of raw physical data averages by wood species measured after stabilisation. Average  $\pm$  standard deviation. For the sake of readability, average values are provided rather than values for each sample.  $\rho_i$  give the density in  $\frac{kg}{m^3}$  at  $i\%$  RH.  $\Delta_{HT_{30-80}}$  and  $\Delta_{DR_{30-80}}$  and represent the relative change in tangential and radial diameters between 30 and 80% RH respectively.  $\frac{T}{R}$  give the ratio between 30 and 80% RH.

Species	$\rho_{50}$ [ $\frac{kg}{m^3}$ ]	$\rho_{80}$ [ $\frac{kg}{m^3}$ ]	$\rho_{30}$ [ $\frac{kg}{m^3}$ ]	$\Delta_{DT_{30-80}}$ [%]	$\Delta_{DR_{30-80}}$ [%]	$\frac{T}{R}$ [-]
<i>A Dalbergia Melanoxylon</i>	NA	NA	NA	NA	NA	NA
<i>B<sub>stab</sub> Fraxinus excelsior</i>	776 $\pm$ 26	783 $\pm$ 26	784 $\pm$ 28	4.4 $\pm$ 0.5	2.0 $\pm$ 0.1	2.2 $\pm$ 0.3
<i>B'<sub>stab</sub> Fraxinus excelsior</i>	826 $\pm$ 13	844 $\pm$ 11	837 $\pm$ 12	3.6 $\pm$ 0.3	1.9 $\pm$ 0.1	1.9 $\pm$ 0.2
<i>B''<sub>stab</sub> Fraxinus excelsior</i>	817 $\pm$ 28	829 $\pm$ 26	821 $\pm$ 24	3.7 $\pm$ 0.2	1.7 $\pm$ 0.1	2.1 $\pm$ 0.2
<i>C<sub>stab</sub> Sequoia sempervirens</i>	531 $\pm$ 44	541 $\pm$ 42	524 $\pm$ 44	2.1 $\pm$ 0.2	1.1 $\pm$ 0.2	2.1 $\pm$ 0.4
<i>D<sub>stab</sub> Prunus avium</i>	749 $\pm$ 110	762 $\pm$ 111	749 $\pm$ 112	3.0 $\pm$ 0.3	1.2 $\pm$ 0.3	2.5 $\pm$ 0.7
<i>E<sub>stab</sub> Fagus sylvatica</i>	975 $\pm$ 53	959 $\pm$ 80	978 $\pm$ 55	4.2 $\pm$ 1.4	3.1 $\pm$ 1.8	1.7 $\pm$ 0.7
<i>F<sub>stab</sub> Cedrus atlantica</i>	798 $\pm$ 8	812 $\pm$ 83	800 $\pm$ 81	3.3 $\pm$ 0.4	1.1 $\pm$ 0.3	3 $\pm$ 0.5
<i>G<sub>stab</sub> Olea europaea</i>	854 $\pm$ 25	893 $\pm$ 27	876 $\pm$ 26	1.5 $\pm$ 0.3	0.6 $\pm$ 0.3	2.9 $\pm$ 0.9
<i>H<sub>stab</sub> Platanus x hispanica</i>	671 $\pm$ 27	681 $\pm$ 29	672 $\pm$ 29	3.2 $\pm$ 0.1	1.7 $\pm$ 0.1	2.0 $\pm$ 0.1
<i>I<sub>stab</sub> Robinia pseudoacacia</i>	741 $\pm$ 6	772 $\pm$ 5	757 $\pm$ 6	1.6 $\pm$ 0.2	1.3 $\pm$ 0.1	1.2 $\pm$ 0.1
<i>J<sub>stab</sub> Carpinus betulus</i>	978 $\pm$ 28	994 $\pm$ 29	986 $\pm$ 29	3.2 $\pm$ 0.2	1.9 $\pm$ 0.2	1.7 $\pm$ 0.2
<i>K<sub>stab</sub> Acer spp.</i>	983 $\pm$ 45	988 $\pm$ 70	993 $\pm$ 45	3.2 $\pm$ 0.2	1.4 $\pm$ 0.1	2.3 $\pm$ 0.2

**Table 9:** Physical properties of samples before and after stabilisation.  $EMC_{50}$  give the equilibrium moisture content of sample at 50% RH, weight percent gain (WPG), moisture exclusion efficiency (MEE) and anti-swelling efficiency (ASE).

Spec	$EMC_{50_{ini}}$ [-] (%)	WPG [-] (%)	$EMC_{50_{stab}}$ [-] (%)	MEE [-] (%)	ASE [-] (%)
<i>A Dalbergia Melanoxylon</i>	4.8±0.4	-	-	-	-
<i>B Fraxinus excelsior</i>	9.2±0.5	14±6	4.5±0.7 (-51%)	44±9	30±7
<i>B' Fraxinus excelsior</i>	9.3±0.5	24±4	4.1±0.2 (-56%)	45±3	17±4
<i>B'' Fraxinus excelsior</i>	9.5±0.4	21±6	4.2±0.7 (-56%)	47±7	28±3
<i>C Sequoia sempervirens</i>	10.9±0.3	31±17	7.7±0.2 (-29%)	13±6	0
<i>D Prunus avium</i>	9.3±0.3	32±16	6.6±0.8 (-29%)	10±5	19±6
<i>E Fagus sylvatica</i>	10.8±0.3	69±10	4.1±1 (-62%)	42±10	42±6
<i>F Cedrus atlantica</i>	10.6±0.4	59±29	5.3±1 (-82%)	21±14	33±3
<i>G Olea europaea</i>	-	-	-	-	-
<i>H Platanus x hispanica</i>	10.3±0.1	8±5	7.5±0.6 (-27%)	21±6	31±3
<i>I Robinia pseudoacacia</i>	9.1±0.3	4±2	1.7±0.2 (-81%)	80±2	52±9
<i>J Carpinus betulus</i>	10.2±0.1	53±5	3.5±0.3 (-66%)	47±5	33±4
<i>K Acer spp.</i>	10.3±0.2	63±5	4.3±0.8 (-58%)	31±1	21±6
<i>L Diospyros crassiflora</i>	6.5±0.8	-	-	-	-

**Table 10:** Average (Avg.) ± standard deviation (SD) of Shore-D hardness before and after stabilisation ( $n = 6$ ), with  $p$ -values from paired  $t$ -tests.

Species	Shore D bef. stab. [-]	Shore D aft. stab. [-]	$p$ -value
<i>A Dalbergia melanoxylon</i>	87±1	-	-
<i>B Fraxinus excelsior</i>	57±3	63±3 (+10.5%)	0.04
<i>B' Fraxinus excelsior</i>	55±2	70±4 (+24%)	0.001
<i>B'' Fraxinus excelsior</i>	55±2	67±3 (+24%)	0.005
<i>C Sequoia sempervirens</i>	39±3	47±5 (+20%)	0.04
<i>D Prunus avium</i>	63±3	69±7 (+9.5%)	0.12
<i>E Fagus sylvatica</i>	65±2	<b>78±5 (+20%)</b>	0.01
<i>F Cedrus atlantica</i>	39±5	64±7 (+64%)	<0.001
<i>G Olea europaea</i>	73±2	75±1 (+3%)	0.29
<i>H Platanus x hispanica</i>	61±2	64±3 (+5%)	0.22
<i>I Robinia pseudoacacia</i>	64±3	76±1 (+19%)	<0.001
<i>J Carpinus betulus</i>	68±1	<b>80±2 (+17%)</b>	<0.001
<i>K Acer sp.</i>	64±4	<b>81±3 (+26.5%)</b>	<0.001
<i>L Diospyros crassiflora</i>	82±2	-	-